MITOR: Jurnal Teknik Elektro

Combining Microstrip Meander Line and Dipole Antennas: Dual-Band Solution for PIR Equipment

Muhamad Adimukti Prasojo[1], Muh Wildan[*,1], Eriyandi[1], Priyo Wibowo[2]
[1]Program Studi Teknik Navigasi Udara – Politeknik Penerbangan Indonesia Curug, [2]BRIN
Tangerang, Indonesia
[*]muh.wildan@ppicurug.ac.id

Abstract – *One of the aviation navigation tools is the Instrument Landing System (ILS), which functions to provide guidance signals to aircraft in the final approach position toward the runway. The ILS consists of three components: the Localizer, Glide Path, and Marker Beacon. To ensure aviation safety and security, navigation equipment must be regularly inspected through Ground Inspection. With current technological advancements, Ground Inspection is being conducted using UAVs or drones. One of the components to be installed on the UAV is the PIR, which requires two antennas of different lengths to receive signals from the Localizer and Glide Path. In this study, a dual-band antenna was developed that combines a dipole antenna and a meander line microstrip antenna for frequencies* 108-112 *MHz and* 328.6-335.4 *MHz, using CST Studio Suite* 2021 *software and FR-4 substrate material. Simulation results showed good performance with a return loss value of* −19.43471 *dB, VSWR of* 1.238951*, and a bandwidth of* 2 *MHz at a frequency of* 110.5 *MHz, and a return loss value of* −27.41626 *dB, VSWR of* 1.119686*, and a bandwidth of* 2.5 *MHz at a frequency of* 329.6 *MHz. Measurement parameter values for the VHF band were a return loss of* −14.1680 *dB, VSWR of* 1.487*, and a bandwidth of* 14.6 *MHz. Meanwhile, for the UHF band, there was a shift in the resonance frequency to* 368.5 *MHz with a return loss value of* −15.4202 *dB, VSWR of* 1.408*, and a bandwidth of* 11.4 *MHz. In this antenna design, a dual-band combination of a dipole and a meander line microstrip antenna with dimensions of* 320 *mm was achieved, capable of operating in both the VHF and UHF frequency bands simultaneously. However, this antenna can only operate at the Localizer working frequency.*

Keywords – *Dual-Band Antenna; Meander Line; Dipole Antenna; PIR Equipment; Ground Inspection.*

I. INTRODUCTION

AVIATION is not just about airplanes flying in the sky. Behind it lies a complex and integrated system consisting of various elements such as airspace, aircraft, airports, air transport, flight navigation, safety and security, the environment, as well as supporting facilities and other public services [1]. Aviation is one of the transportation modes that offers high speed and safety. As the demand for air travel increases, safety guarantees must also be continually enhanced [2]. Therefore, high-quality and optimal aviation safety equipment is necessary to support fast, safe, and comfortable air travel.

The main obstacle in aircraft landing is adverse weather conditions such as fog, dew, and rain [3]. These conditions make it difficult for airplanes to land accurately. Therefore, aviation navigation equipment is needed to support flight safety [4]. Flight navigation is an essential aspect of aviation that ensures the safety and smooth operation of air travel. By mastering the art and science of navigation, pilots can deliver their passengers and cargo to their destinations safely and on time [5]. Flight navigation is crucial to ensuring that aircraft can fly safely to their destination. It acts as a guide and direction for pilots with the goal of ensuring safety at every stage of flight, from takeoff, during the journey in the air, until landing at the destination airport.

One of the aviation navigation systems is the Instrument Landing System (ILS). The ILS is a flight navigation tool that provides guiding signals to aircraft during the final approach to the runway. The ILS is an infrastructure that supports airport operations, ensuring that aircraft can land safely and comfortably, especially under low-visibility conditions caused by fog or rain [6]. The ILS has three components: the Localizer, Glide Path, and Marker Beacon. The Localizer operates in the VHF frequency band between 108 MHz

The manuscript was received on August 19, 2024, revised on November 1, 2024, and published online on November 29, 2024. `Emitor` is a Journal of Electrical Engineering at Universitas Muhammadiyah Surakarta with ISSN (Print) 1411 – 8890 and ISSN (Online) 2541 – 4518, holding Sinta 3 accreditation. It is accessible at https://journals2.ums.ac.id/index.php/emitor/index.

– 112 MHz to guide the aircraft to the runway centerline. The Glide Path operates in the UHF frequency band between 328.6 MHz – 335.4 MHz to guide the landing angle at 3 degrees. The Marker Beacon operates on a single frequency of 75 MHz, which is used to determine the distance from the threshold [7].

To ensure aviation safety and security, the performance of aviation navigation equipment must be inspected regularly from the ground (Ground Inspection) [8]. The purpose of this activity is to assess the signal emission parameters of the Localizer and Glide Path equipment, including DDM, SDM, RF Level, and Different Level values. This activity requires the use of a Portable ILS/DVOR Receiver (PIR) to measure the signal emission parameters of the Localizer and Glide Path. The Ground Inspection of the Localizer can be performed by measuring the signal emission parameters at pre-determined horizontal points. However, there are challenges in checking the Glide Path signal parameters due to its vertical emission, which needs to be measured using poles typically no higher than about 25 meters from the ground, making manual Ground Inspection impossible. Therefore, with current technological advancements, Ground Inspection using Unmanned Aerial Vehicles (UAVs) or drones is proposed.

The use of Unmanned Aerial Vehicles or drones for Ground Inspection will simplify the process and address previous issues [9]. The results of this activity can be immediately obtained through a laptop display showing real-time parameter data, allowing for immediate evaluation to determine whether the standards have been met. The construction of UAVs or drones is divided into several parts, such as the Drone GPS Antenna, RTK Data Link, PIR, camera, and data display software. One of the components of the UAV is the PIR, which requires two antennas of different lengths to receive signals from the Localizer and Glide Path. This is due to the different operating frequencies between the Localizer and Glide Path equipment, necessitating the use of antennas that match their respective frequency bands [10]. Therefore, an antenna with dual-band frequencies, namely Very High Frequency (VHF) and Ultra High Frequency (UHF), is needed to receive signals from both the Localizer and Glide Path simultaneously. Additionally, a small antenna design is required to be used and mounted on the drone [11].

As the foundation for this research, the antenna design in this study uses several methods previously researched by other researchers, which are needed to design a combination of microstrip and dipole dual-band frequency antennas. The study conducted by Juan Ronaldo Sianipar et al. [12] resulted in a microstrip meander line antenna operating at a central frequency of 329.6 MHz with a VSWR of 1.23, return loss of -19.65 dB, bandwidth of 7.3 MHz, and dimensions of 150 mm x 50 mm. In another study by E. Yovita et al. [13], a Dual Band Rectangular Patch Microstrip Antenna with Slots was designed, operating at frequencies of 2.6 GHz and 5 GHz. For the 2.6 GHz frequency, the antenna achieved a VSWR of 1.092, return loss of -27.1 dB, and a bandwidth of 38 MHz, while for the 5 GHz frequency, the antenna achieved a VSWR of 1.411, return loss of -15.3 dB, and a bandwidth of 124 MHz. Another study by A. Muhammad Nashrullah et al. [14] designed a microstrip meander line antenna operating at 924 MHz with a VSWR of 1.363, return loss of -16.262 dB, and a bandwidth of 21.659 MHz. Further research by M. Arpaio et al. [15] designed a dual-band antenna for ADSB applications with a frequency range of 1.030–1.090 GHz and 5G communications with a frequency range of 3.4–3.8 GHz using two substrate materials, aluminum and FR-4. Another study conducted by Muhamad Adimukti Prasojo et al. [16] investigated the influence of changes in ground plane dimensions and line length on a 332 MHz meander line microstrip antenna. The results indicate that variations in ground plane dimensions and patch line length on the meander line microstrip antenna affect the antenna's performance.

Based on these studies, the researchers designed an antenna combining a dipole antenna and a dual-band microstrip meander line antenna for operating frequencies of 108–112 MHz and 328.6–335.4 MHz. This design is expected to produce an antenna with dual-band frequencies that can be used by both ILS devices, namely the Localizer and Glide Path, simultaneously. Additionally, this design is expected to create a minimalistic antenna to facilitate its operation. The authors aim for the design parameters to achieve a return loss of ≤ -10 dB and a VSWR of < 2.

II. Research Methods

The ADDIE method was chosen for this research because it offers systematic stages in its workflow. This method uses a scientific approach to gather data for specific purposes and objectives [17]. The ADDIE method consists of five stages:

1. Analysis. In this stage, the researcher conducts a literature review to identify key parameters that will serve as references for the antenna design being developed.
2. Design. At this stage, the shape and dimensions of the antenna are designed using CST Studio Suite 2021 software. After the design process, simula-

tions are conducted to evaluate the performance of the designed antenna.

3. Development. Following the simulation, the next step is to fabricate the designed antenna. The results from this process undergo parameter testing to assess the antenna's physical performance.
4. Implementation. During this stage, the parameters of the fabricated antenna are measured and compared with the simulation results to assess its ability to receive signals from the Localizer and Glide Path.
5. Evaluation. Finally, the researcher evaluates the measurement results to determine whether the parameters meet the planned specifications.

A structured and systematic approach is required when designing the antenna to ensure an efficient research process in terms of production costs and design time. The flowchart of the antenna design process is shown in Figure 1.

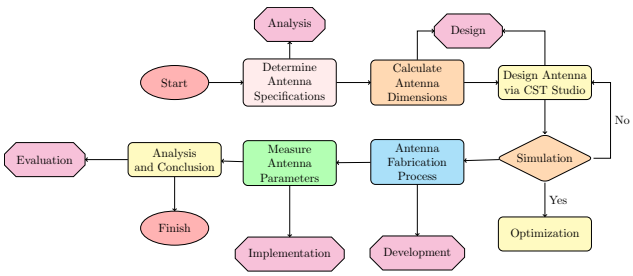

Figure 1: Flowchart of Antenna Design

The following is the antenna system design used for PIR reception, shown in Figure 2.

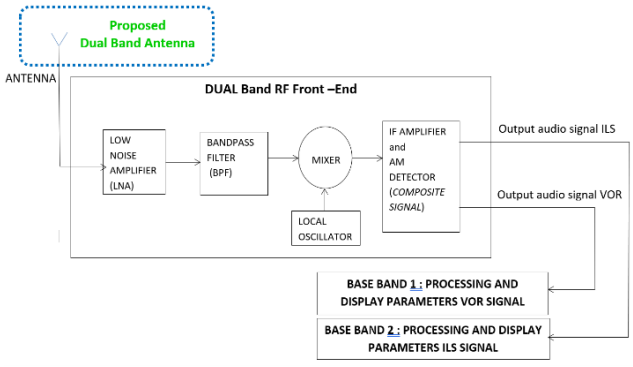

Figure 2: RF Diagram on PIR and Proposed Dual-Band Antenna Design

Below are the substrate parameters used in the design of the microstrip meander line and dipole antenna combination, as shown in Table 1.

To operate at frequencies of 108-112 MHz and 328.6 – 335.4 MHz, the antenna design must meet the desired performance characteristics. The specifications are outlined in Table 2.

Table 1: Substrate Specifications

Substrate Type	FR-4 Epoxy
Dielectric Constant	4.4
Substrate Thickness	1.6 mm
Patch Thickness	0.0035 mm

Table 2: Antenna Specifications

Parameter	Value
Operating Frequency	108-112 MHz & 328.6-335.4 MHz
Central Frequency	110.5 MHz & 329.6 MHz
Terminal Impedance	50 Ω (coaxial connector SMA)
VSWR	< 2
Return Loss	< -10 dB

III. Results and Discussion

In this design, a combination of dipole and microstrip meander line dual-band antennas is used to operate at 110.5 MHz and 329.6 MHz, with the goal of reducing the antenna size for low frequencies. The design specifications of the antenna are as follows:

1. Dipole Antenna
   (a) Material: Copper
   (b) Method: Folded-end dipole
2. Microstrip Antenna
   (a) Substrate Material: FR-4 Epoxy
   (b) Substrate Thickness: 1.6 mm
   (c) Permittivity (ε_r): 4.3
   (d) Patch Method: Meander line
   (e) Patch Material: Copper
   (f) Patch Thickness: 0.035 mm
   (g) Operating Frequency: 108 MHz – 118 MHz & 328.6 MHz - 335.4 MHz

In the initial design steps, several antenna parameters were established as a basis for the design. These initial parameters can be seen in Table 3.

Table 3: Initial Antenna Parameters

Parameter	Value
Central Frequency	110.5 MHz & 329.6 MHz
Return Loss	¡ -10 dB
VSWR	≤ 2
Bandwidth	MHz & 6.8 MHz

In the substrate material selection process, determining the permittivity value of the material is the main factor. There are various substrate options with different permittivity values. For this research, FR-4 Epoxy substrate with a permittivity value (ε_r) of 4.3 and a thickness of 1.6 mm was chosen due to its wide

availability in the market and its moderate permittivity value. Meanwhile, the material used for the patch layer, ground plane, and the dipole antenna construction in this study is copper. Copper was chosen for its ability to efficiently radiate electromagnetic waves and its compatibility with FR-4 substrate as an electromagnetic wave reflector. The thickness of the copper for the patch and ground plane is 0.035 mm. Meanwhile, the diameter of the dipole antenna will be determined after calculations are completed.

i. Calculation of Dimensions and Antenna Length

Before determining the length of the antenna, the first step is to calculate the wavelength for frequencies of 110.5 MHz (λ_1) and 329.6 MHz (λ_2). The wavelength calculation can be formulated through Equation (1) [18, 19].

$$\lambda = \frac{c}{f_c} \tag{1}$$

with:

$$\lambda_1 = \frac{c}{f_1} = \frac{3\times10^8}{110.5\times10^6} = 2.71493 \text{ m}$$
$$\lambda_2 = \frac{c}{f_2} = \frac{3\times10^8}{329.6\times10^6} = 0.91094 \text{ m}$$

Based on the calculations above, the wavelength value for a frequency of 110.5 MHz is 2.71493 meters, and the wavelength for a frequency of 329.6 MHz is 0.91094 meters.

After obtaining the wavelength for each frequency, the antenna length can be calculated by applying formula (2) with $K = 0.95$ (velocity factor for metal).

$$L = K \times \frac{\lambda}{2} \tag{2}$$

with: Length of the dipole antenna for 110.5 MHz:

$$L_{\frac{1}{2}\text{vhf}} = K \times \frac{1}{2}\lambda = 0.95 \times \frac{1}{2} \times 2.71493 = 1.29 \text{ m}$$

Length of the dipole antenna for 329.6 MHz:

$$L_{\frac{1}{2}\text{uhf}} = K \times \frac{1}{2}\lambda = 0.95 \times \frac{1}{2} \times 0.91094 = 0.43 \text{ m}$$

The total antenna length for these two frequencies is:

$$L = \frac{L_{\frac{1}{2}\text{vhf}} + L_{\frac{1}{2}\text{uhf}}}{2} = \frac{1.29+0.43}{2} = 0.86 \text{ m} \tag{3}$$

From this total antenna length, it will be divided into 2 parts, with half of the total antenna length being made into a folded end dipole antenna and half of the other length transformed into a microstrip meander line antenna.

Dipole Antenna Length (L_1)

$$L_1 = \frac{1}{2} \times 0.86 = 0.43 \text{ m} = 430 \text{ mm} \tag{4}$$

Antenna Length after Bending

$$L_2 = \frac{\text{Distance of side}}{2} = \frac{430}{2} = 215 \text{ mm} \tag{5}$$

The diameter of the dipole antenna can be calculated using the following formula:

$$R = \frac{\lambda}{1000} = \frac{2.714}{1000} = 2.7 \text{ mm} \tag{6}$$

ii. Microstrip Meander Line Antenna Dimension

The dimensions of the substrate in the meander line antenna are related to the number of lines on the antenna patch. The more lines there are, the larger the substrate dimensions needed. Meanwhile, the size of the ground plane for the microstrip meander line antenna is not determined by a standard, but is obtained through an optimization process. The initial size of the ground plane is generally taken to be 100% of the length of the substrate, then optimized to achieve maximum antenna performance.

A microstrip antenna is said to be matched when the transmission line impedance (Z_0) is equal to the load impedance (Z_1) [20]. Z_0 generally has a value of 50 Ω, while Z_1 is the impedance of the microstrip antenna. The microstrip antenna is supplied by a feed with an impedance of 50 Ω and an SMA female connector. To calculate the feed width with an impedance of 50 Ω, formulas in equations (7) and (8) can be used [14].

$$B = \frac{60\pi^2}{Z_0\sqrt{\varepsilon_r}} = \frac{60\times(3.14)^2}{50\sqrt{4.3}} = 5.7 \tag{7}$$

$$W_f = \frac{2h}{\pi}\left\{B - 1 - \ln(2B-1) + \frac{\varepsilon_r - 1}{2\varepsilon_r}\left[\ln(2B-1) + 0.39 - \frac{0.61}{\varepsilon_r}\right]\right\} \tag{8}$$

Calculating W_f:

$$W_f = \frac{2\times1.6}{3.14}\left\{5.7 - 1 - \ln(2\times5.7-1) + \frac{4.3-1}{2\times4.3}\left[\ln(2\times5.7-1) + 0.39 - \frac{0.61}{4.3}\right]\right\} = 2.7 \text{ mm} \tag{9}$$

Next, to calculate the length of the feedline using the following equation [21]:

$$\frac{W_f}{h} = \frac{2.7}{1.6} = 1.6875 > 1$$

Since $\frac{W_f}{h} > 1$, the effective dielectric constant (ε_{eff}) can be calculated using formula (10).

$$\varepsilon_{\text{eff}} = \frac{\varepsilon_r + 1}{2} + \frac{\varepsilon_r - 1}{2}\left\{\frac{1}{\sqrt{1+\frac{12\times h}{w}}}\right\} \quad (10)$$

Calculating ε_{eff}:

$$\varepsilon_{\text{eff}} = \frac{4.3+1}{2} + \frac{4.3-1}{2}\left\{\frac{1}{\sqrt{1+\frac{12\times 1.6}{2.7}}}\right\}$$
$$= 2.65 + 1.65 \times 0.3511 = 3.22$$

After finding the value of the dielectric constant (ε_{eff}), use equations (11) and (12) to find the value of the feedline length.

$$l_f = \frac{\lambda_d}{4} \quad (11)$$

$$\lambda_d = \frac{\lambda}{\sqrt{\varepsilon_{\text{eff}}}} = \frac{903}{\sqrt{3.22}} = 280.434 \text{ mm} \quad (12)$$

Thus, the length of the feedline is:

$$l_f = \frac{280.434}{4} = 70.1 \text{ mm}$$

The parameter values for the lines in the meander line antenna begin with adjustments according to the length and width of the feedline. This is done as a preliminary step in the antenna design process. Adjusting the line parameters aims to achieve impedance matching between the antenna and the feedline [22]. This is crucial to ensure optimal power transfer from the signal source to the antenna.

$$l_i = \frac{l_f}{2} = \frac{70.1}{2} = 35.05 \text{ mm}$$
$$W_i = W_f = 2.7 \text{ mm}$$

Based on the calculations, the length of the meander line antenna (l_l) is found to be 35.05 mm and the line width (W_l) is 2.7 mm. Meanwhile, the spacing between lines is adjusted according to the feedline width, which is $l_{\text{gap}} = W_f = 2.7$ mm. The number of lines in the microstrip antenna at a certain frequency can be calculated using the following formula:

$$N = \frac{L}{L_i + W_i} = \frac{1260}{35.05 + 2.7} = 34 \text{ lines} \quad (13)$$

Based on all the calculations above, the initial data for the combined dipole antenna and microstrip meander line antenna can be seen in Table 4.

Table 4: Initial Antenna Dimensions

Parameter	Symbol	Size
Dipole antenna length	L_1	430 mm
Antenna length after bending	L_2	215 mm
Dipole antenna diameter	R	2.7 mm
Feedline length	l_f	70.1 mm
Feedline width	W_f	2.7 mm
Line length	l_i	35.05 mm
Line width	W_i	2.7 mm
Distance between lines	l_{gap}	2.7 mm
Number of lines	N	34
Substrate length	P_s	450 mm
Substrate width	L_s	50 mm
Ground plane length	P_g	450 mm
Ground plane width	L_g	50 mm
Patch thickness	T_p	0.035 mm
Substrate thickness	T_s	1.6 mm

iii. Antenna Design Simulation

The antenna design simulation was conducted using CST Studio Suite 2021 software to determine the initial antenna parameters based on the previous calculations. Below are the results of the initial simulation of the combined dipole antenna and microstrip meander line antenna design.

(a)

(b)

Figure 3: Initial Antenna Design (a) Front View and (b) Back View

From the images above, the simulation results of the initial design parameters for the combined dipole and microstrip meander line antennas are shown in Figure 4 below.

Based on Figure 4, the best parameter results were at the center frequency of 150.5 MHz with a return loss value of -35.4377 dB and a VSWR of 1.034399, and at the center frequency of 310 MHz with a return loss value of -11.4573 dB and a VSWR of 1.729942. However, these results did not meet the desired specifications, which were to operate at center frequencies of 110.5 MHz and 329.6 MHz. Therefore, the antenna

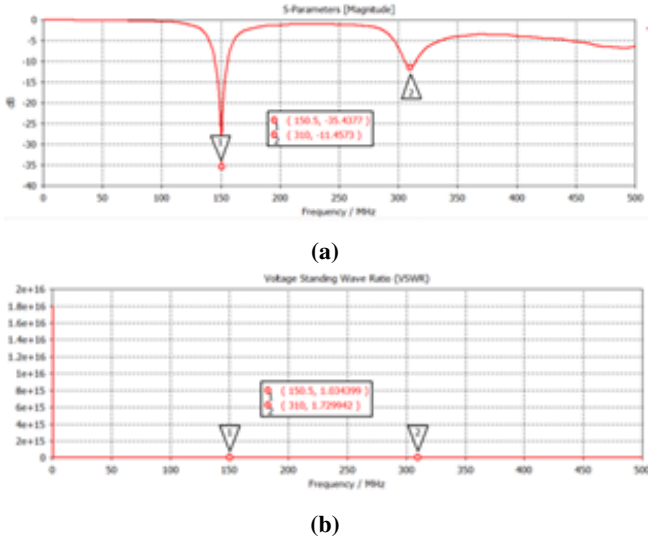

(a)

(b)

Figure 4: Return Loss (a) and VSWR (b) Parameters of the Initial Design

design needs to be optimized to achieve the expected specifications with better parameter values.

iv. Antenna Design Optimization

The antenna design optimization was carried out by adjusting the initial antenna dimensions, such as changing the dimensions of the ground plane, substrate dimensions, line length, dipole antenna length, and other factors until the desired parameter results were achieved. The final design after antenna optimization can be seen in Figure 5 below.

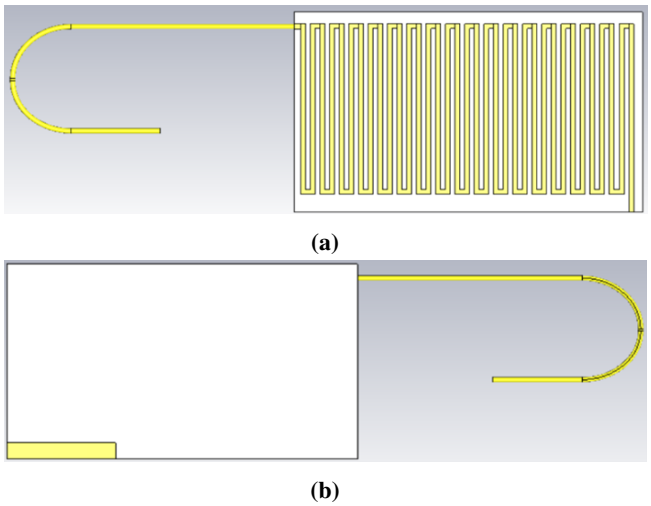

(a)

(b)

Figure 5: Optimized Antenna Design (a) Front View and (b) Back View

Based on the optimized antenna design, several parts experienced reductions or increases in dimension sizes. The parts that saw reductions in size include the dipole antenna length, antenna length after bending, substrate length, and ground plane dimensions. Meanwhile, the parts that saw increases in size include the dipole antenna diameter, feedline length, line length, and substrate width. The comparison of dimensions before and after optimization can be seen in Table 5.

Table 5: Comparison of Antenna Dimensions Before and After Optimization

Parameter	Before Optimization (mm)	After Optimization (mm)	Difference (%)
Dipole antenna length	430	125	-54.95
Antenna length after bending	215	50	-62.26
Dipole antenna diameter	2.7	3	+5.26
Feedline length	70.1	108.2	+21.37
Feedline width	2.7	2.7	0
Line length	35.05	98	+47.31
Line width	2.7	2.7	0
Distance between lines	2.7	2.7	0
Number of lines	34	34	0
Substrate length	450	195	-39.53
Substrate width	50	115	+39.39
Ground plane length	450	60.5	-76.30
Ground plane width	50	9.4	-68.35
Patch thickness	0.035	0.035	0
Substrate thickness	1.6	1.6	0

Notes:

- The (+) sign indicates an increase in antenna dimension size.
- The (-) sign indicates a decrease in antenna dimension size.

After optimizing the design of the combined dipole antenna and microstrip meander line antenna, the resulting parameters such as return loss and VSWR can be seen in Figure 6 below.

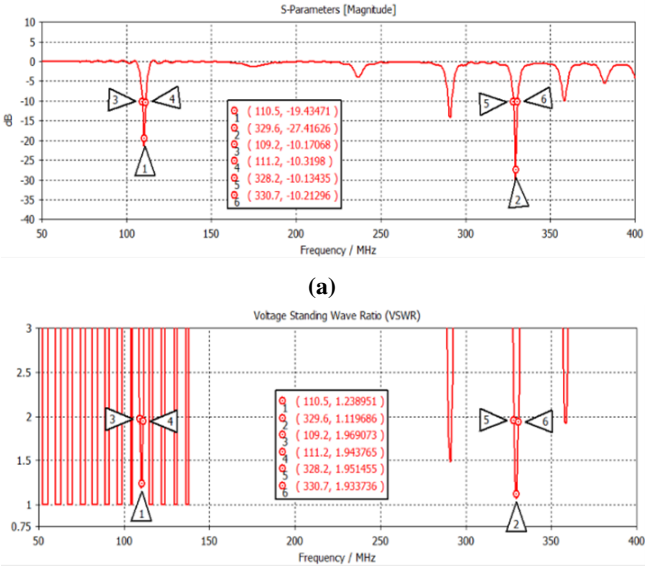

(a)

(b)

Figure 6: Simulation Results After Optimization (a) Return Loss Value and (b) VSWR Value

v. Antenna Design Simulation Results

The provided data shows that the combined dipole and microstrip meander line antenna design can resonate at several frequencies, including the desired frequencies of 110.5 MHz and 329.6 MHz. The information

includes the return loss (S_{11}) and VSWR parameters. From this data, information about the operational frequency and bandwidth of this antenna design can be obtained. This is based on simulation results using CST Studio Suite 2019 software, which shows that the antenna can operate in the frequency range of 109.2 MHz to 111.2 MHz with a bandwidth of 2 MHz, a VSWR of 1.238951, and a return loss of -19.43471 dB at the center frequency of 110.5 MHz. Additionally, in the frequency range of 328.2 MHz to 330.7 MHz, the antenna achieved a bandwidth of 2.5 MHz, a VSWR of 1.119686, and a return loss of -27.41626 dB at the center frequency of 329.6 MHz. The return loss and VSWR values from the simulation can be seen in Table 6.

Table 6: Parameter Values of the Simulation Results After Optimization

Marker	Frequency (MHz)	Return Loss (dB)	VSWR
M1	110.5	-19.43471	1.238951
M2	329.6	-27.41626	1.119686
M3	109.2	-10.17068	1.969073
M4	111.2	-10.3198	1.943765
M5	328.2	-10.13435	1.951455
M6	330.7	-10.21296	1.933736

Based on this final simulation, it can be seen that the impedance values match the expected impedance values, which are close to 50 Ω. Below is a graph showing the impedance values from the final simulation:

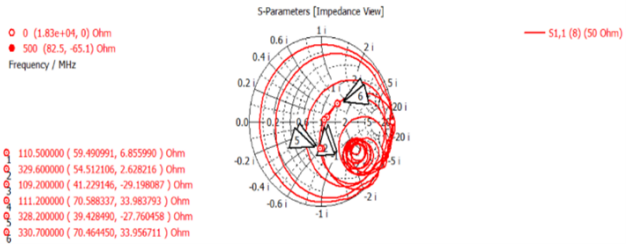

Figure 7: Impedance Graph After Optimization

The impedance obtained from the simulation is $59.490991 + j6.855990\ \Omega$ at a frequency of 110.5 MHz and $54.512106 + j2.62916\ \Omega$ at a frequency of 329.6 MHz.

The simulation also provides information on the radiation pattern generated, which visually illustrates the far-field radiation characteristics of the antenna, depending on the specific direction of the antenna design [23]. The radiation pattern results can be seen in Figure 8 below.

From the images above, it can be seen that the radiation pattern cuts produce a bidirectional pattern for the VHF band and a directional pattern for the UHF band. The overall final parameters after optimization

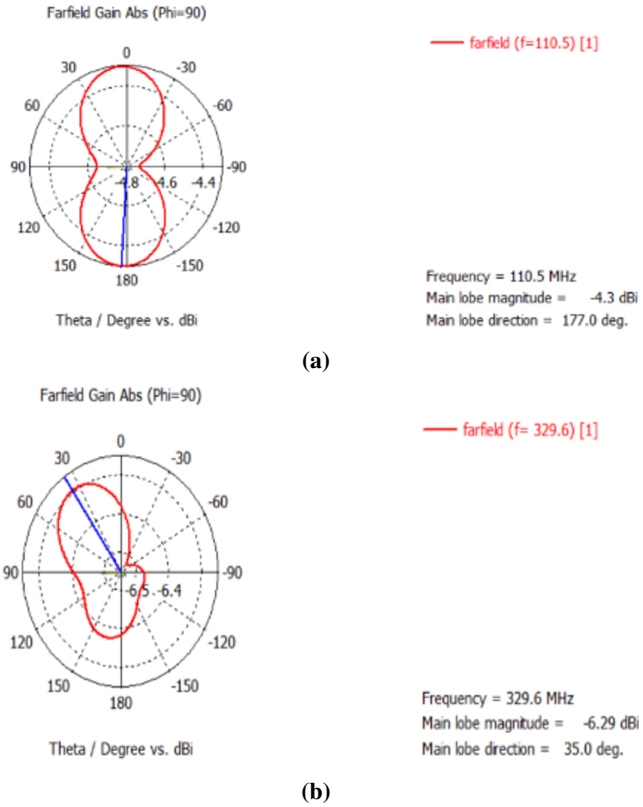

Figure 8: Radiation Pattern Results After Optimization (a) Frequency 110.5 MHz and (b) Frequency 329.6 MHz

can be seen in Table 7.

Table 7: Final Simulation Results After Optimization

Specification	Frequency 110.5 MHz	Frequency 329.6 MHz
Return loss	-19.43471 dB	-27.41626 dB
VSWR	1.238951	1.119686
Bandwidth	2 MHz	2.5 MHz
Impedance	$59.490991 + j6.855990\ \Omega$	$54.512106 + j2.62916\ \Omega$
Radiation Pattern	Bidirectional	Directional

vi. Development Stage

After completing the antenna design and ensuring that the parameters meet the standards through software testing, the next step is fabrication. The designed antenna will be made using an FR-4 PCB substrate measuring 195 mm x 115 mm. The dipole antenna will be fabricated using 3 mm diameter copper wire, with the dipole antenna length being 125 mm and the length after bending being 5 mm. The bent dipole antenna will then be connected to the microstrip meander line antenna using soldered tin. This dual-band dipole and microstrip meander line antenna assembly will be fitted with an SMA-Female connector. The fabricated antenna results are shown in Figure 9.

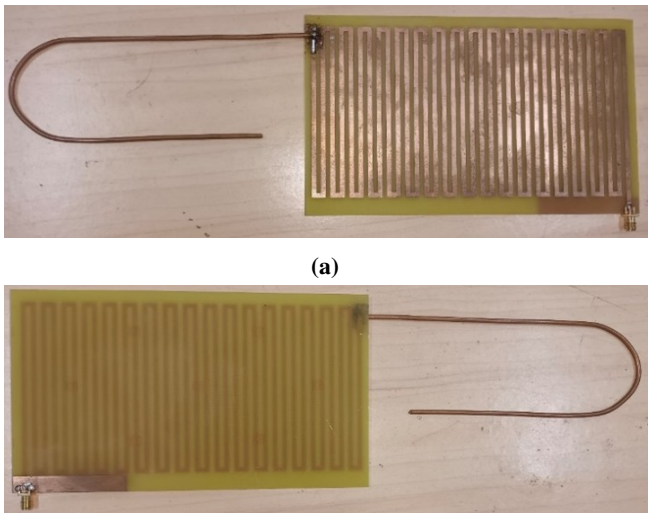

(a)

(b)

Figure 9: Fabricated Antenna (a) Front View and (b) Back View

vii. Implementation Stage

Antenna Measurement Procedure. Testing or measurement will be conducted on the printed antenna to compare the parameters from the simulation using CST Studio Suite 2021 with the fabricated antenna. The parameters being compared include return loss, VSWR, bandwidth, and impedance. The measurement will use a Rohde & Schwarz ZNC 3 Vector Network Analyzer in the Advanced Laboratory of the Aerospace Engineering Department.

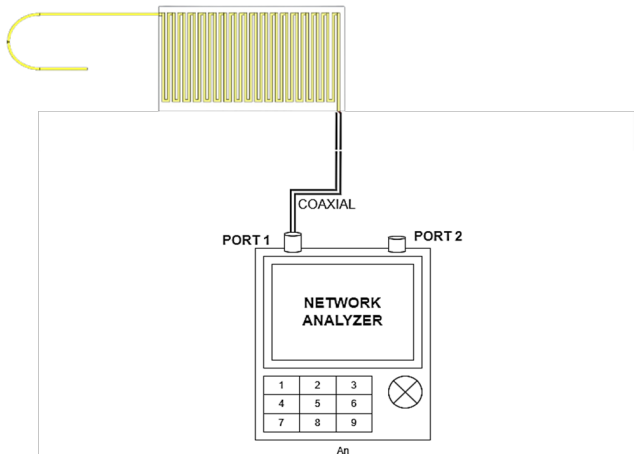

Figure 10: Measurement Setup Using Vector Network Analyzer Rohde & Schwarz ZNC 3

The flow diagram for the antenna measurement procedure using the Vector Network Analyzer Rohde & Schwarz ZNC 3 can be seen in Figure 11.

Antenna Measurement Results. After measuring the combined dual-band dipole and microstrip meander line antenna, the following parameters were obtained:

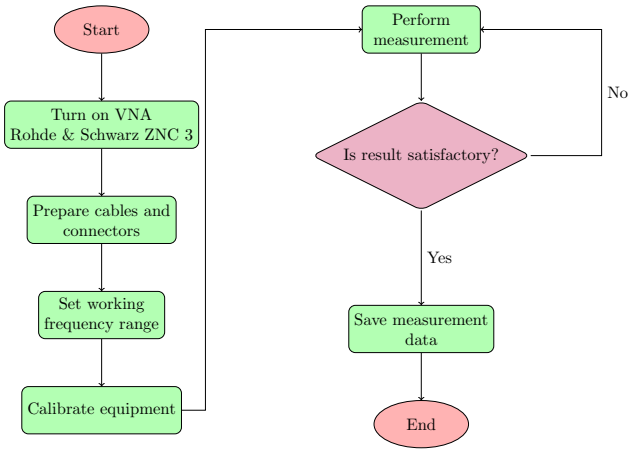

Figure 11: Flow Diagram of the Antenna Measurement Procedure

viii. Return Loss

Return loss is measured to assess the reflection coefficient, indicating how much power is lost due to a mismatch between the antenna and the transmission line [24]. The lower the return loss, the less power is lost at the antenna, meaning better antenna performance. Below are the return loss measurements using the Vector Network Analyzer Rohde & Schwarz ZNC 3.

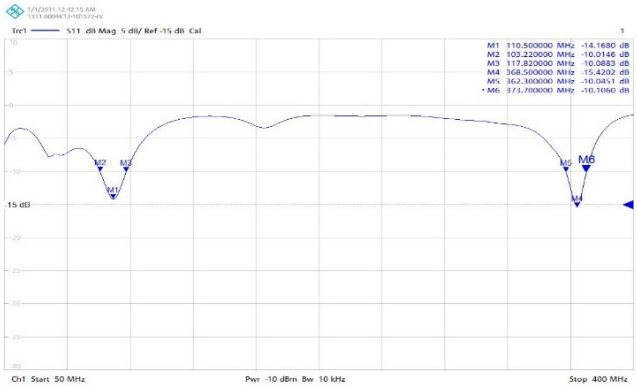

Figure 12: Return Loss Measurement Graph

The graph shows that the return loss at the VHF and UHF working frequencies has been obtained. For the VHF frequency, the lowest return loss was recorded at 110.50 MHz at marker 1 (M1) with a value of -14.1680 dB, with the lower limit at 103.22 MHz at marker 2 (M2) with a value of -10.0146 dB, and the upper limit at 117.82 MHz at marker 3 (M3) with a value of -10.0883 dB. At the UHF frequency, the lowest return loss was found at 368.50 MHz at marker 4 (M4) with a value of -15.4202 dB, with the lower limit at 362.30 MHz at marker 5 (M5) with a value of -10.0451 dB, and the upper limit at 373.70 MHz at marker 6 (M6) with a value of -10.1060 dB.

ix. VSWR Value

VSWR (Voltage Standing Wave Ratio) is measured to determine the ratio between maximum and minimum voltage in the standing wave generated by the reflection due to impedance mismatch between the antenna input and the transmission line. Higher VSWR values indicate greater reflected power, which can damage equipment. Below are the VSWR measurement results using the Vector Network Analyzer Rohde & Schwarz ZNC 3.

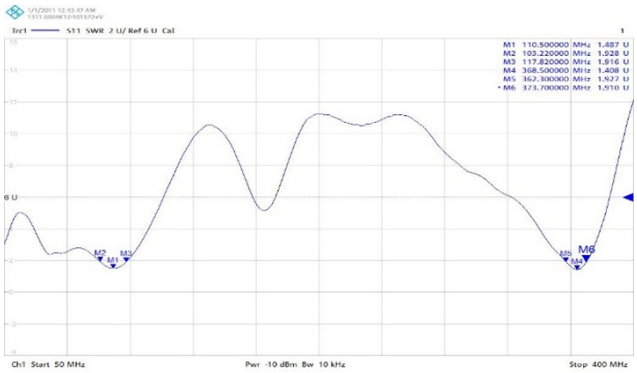

Figure 13: VSWR Measurement Graph

From the graph, the VSWR values at the VHF and UHF working frequencies can be seen. At the VHF frequency, the lowest VSWR was recorded at 110.50 MHz at marker 1 (M1) with a value of 1.487. The lower limit was at 103.22 MHz at marker 2 (M2) with a value of 1.928, and the upper limit at 117.82 MHz at marker 3 (M3) with a value of 1.916. At the UHF frequency, the lowest VSWR was recorded at 368.50 MHz at marker 4 (M4) with a value of 1.408, with the lower limit at 362.30 MHz at marker 5 (M5) with a value of 1.927, and the upper limit at 373.70 MHz at marker 6 (M6) with a value of 1.910.

x. Impedance Value

This impedance measurement is essential because it affects the match between the transmission line and the antenna. The measurement results show that the antenna impedance matches the expected specification, approximately $\pm 50\ \Omega$. Below are the impedance measurement results using the Vector Network Analyzer Rohde & Schwarz ZNC 3.

Based on the graph above, the impedance values at the VHF and UHF working frequencies can be found. At the VHF frequency, the lowest impedance was recorded at 110.50 MHz at marker 1 (M1) with a value of 60.402 Ω, with the lower limit at 103.22 MHz at marker 2 (M2) with a value of 46.015 Ω and the upper limit at 117.82 MHz at marker 3 (M3) with a value of 88.709 Ω. At the UHF frequency, the lowest

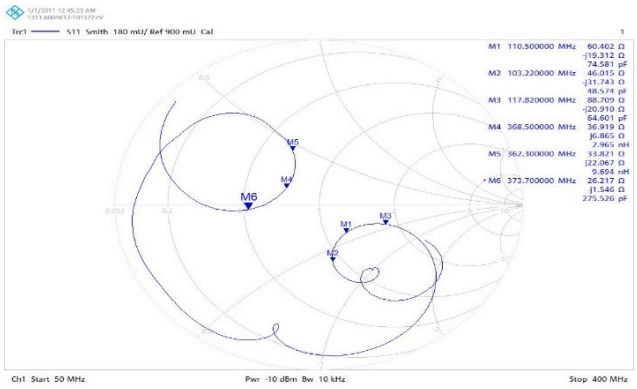

Figure 14: Impedance Measurement Graph

impedance was recorded at 368.50 MHz at marker 4 (M4) with a value of 36.919 Ω, with the lower limit at 362.30 MHz at marker 5 (M5) with a value of 33.821 Ω and the upper limit at 373.70 MHz at marker 6 (M6) with a value of 26.217 Ω.

xi. Bandwidth Value

Bandwidth can be measured using the return loss or VSWR graph of the tested antenna. An antenna is considered to operate well if the return loss value is $\leq$ -10 dB and the VSWR value is < 2. Based on this criterion, the bandwidth can be calculated using the Equation (14).

$$\text{Bw} = F_2 - F_1 \tag{14}$$

Bandwidth VHF

$$\text{Bw VHF} = 117.82\ \text{MHz} - 103.22\ \text{MHz} = 14.60\ \text{MHz}$$

Bandwidth UHF

$$\text{Bw UHF} = 373.70\ \text{MHz} - 362.30\ \text{MHz} = 11.40\ \text{MHz}$$

The measurement results show a bandwidth of 14.6 MHz at the VHF frequency and 11.4 MHz at the UHF frequency, meeting the specified requirements of 4 MHz for VHF and 6.8 MHz for UHF. For percentage calculation, it can be computed using the equation:

$$\%\text{Bw} = \frac{F_2 - F_1}{F_C} \times 100\%$$

Percentage Bandwidth VHF

$$\%\text{Bw VHF} = \frac{117.82 - 103.22}{110.52} \times 100\% = 13.21\%$$

Percentage Bandwidth UHF

$$\%\text{Bw UHF} = \frac{373.70 - 362.30}{368} \times 100\% = 3.09\%$$

xii. Evaluation Stage

After the measurement using the Vector Network Analyzer Rohde & Schwarz ZNC 3, the following comparisons between simulation and measurement were obtained:

Table 8: Comparison of VHF and UHF Simulation and Measurement Results

Parameter	Specification	Simulation	Measurement	Result
VHF Frequency Band				
Frequency Operation	108 - 112 MHz	109.2 – 111.2 MHz	103.22 - 117.82 MHz	M
Return Loss	¡ -10 dB	-19.43471 dB	-14.1680 dB	M
VSWR	¡ 2	1.238951	1.487	M
Bandwidth	4 MHz	2 MHz	14.6 MHz	M
Impedance	±50 Ω	59.49 Ω	60.402 Ω	M
UHF Frequency Band				
Frequency Operation	328.6 – 335.4 MHz	328.2 – 330.7 MHz	362.3 - 373.7 MHz	DM
Return Loss	¡ -10 dB	-27.41626 dB	-15.4202 dB	M
VSWR	¡ 2	1.119686	1.408	M
Bandwidth	6.8 MHz	2.5 MHz	11.4 MHz	M
Impedance	±50 Ω	54.51 Ω	36.919 Ω	DM

Notes: *M* = Meets the requirements, *DM* = Doesn't Meet the requirements.

The following shows a comparison graph of return loss and VSWR values between the simulation results and the measurement results.

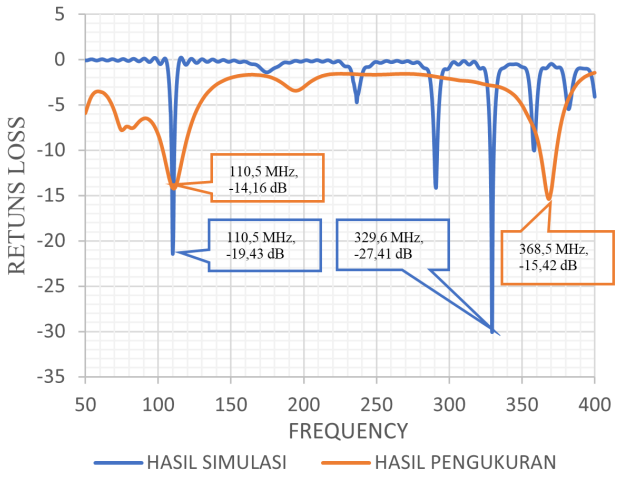

Figure 15: Comparison Graph of Return Loss Simulation and Measurement Results

Based on Figures 15 and 16, it is evident that there are differences between the simulation and measurement results of the antenna performance. This occurs because the measurement was conducted in an environment with an unstable radiation field distribution. In the VHF frequency band, the simulation results yielded a return loss value of -19.43 dB at a frequency of 110.5 MHz. Meanwhile, the measurement yielded a return loss value of -14.16 dB at the same resonance frequency as the simulation, which is 110.5 MHz. In the UHF frequency band, the simulation produced a return loss value of -27.41 dB at a resonance frequency of 329.6 MHz, while the best return loss value in the measurements shifted to 368.5 MHz, with a value of 15.42

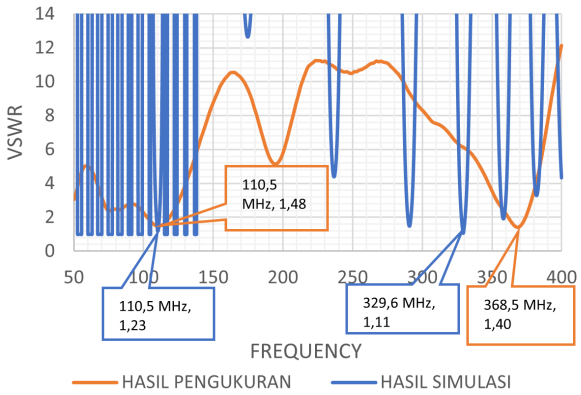

Figure 16: Comparison Graph of VSWR Simulation and Measurement Results

dB. This frequency shift is caused by several factors, including:

1. Environmental influence from objects around the measurement area.
2. The quality of the dielectric material.
3. Accuracy in the PCB etching process.
4. Human or machine errors during fabrication.
5. Measurement tool accuracy.
6. The quality of cables and connectors.
7. Differences in impedance in the cables or connectors used, which can cause discrepancies between the measurement and simulation results.

Although the return loss and VSWR values decreased compared to the simulation results, the fabricated bandwidth for the VHF band met the specified requirements, which is 14.6 MHz. Meanwhile, in the UHF frequency band, the bandwidth achieved was 11.4 MHz, but its resonance frequency shifted from the simulation results. Therefore, the measurement results after fabrication still require optimization to operate on both the Localizer and Glide Path working frequencies simultaneously. This means that the antenna is not yet ready to be tested using PIR.

IV. Conclusion

Based on the design results, a combination of a dipole antenna and a dual-band microstrip meander line antenna was created, which can operate simultaneously in the VHF and UHF frequency bands. However, this antenna can only function in the Localizer operating frequency due to a frequency shift in the UHF band, making it unable to operate at the Glide Path frequency. Additionally, the antenna design has return loss values of -14.1680 dB and -15.4202 dB and VSWR values of 1.487 and 1.408 at center frequencies of 110.5 MHz and 368.5 MHz, respectively. These parameters meet the expected specifications of having a return loss of

< -10 dB and VSWR < 2. On the other hand, the antenna's dimensions are 195 mm x 115 mm for the microstrip antenna and 125 mm in length on the top side and 50 mm on the bottom side for the dipole antenna, resulting in a total antenna length of 320 mm. These dimensions allow the antenna to be mounted on a drone, although it can only operate in the Localizer frequency range.

References

[1] R. Indonesia, "Peraturan pemerintah republik indonesia nomor 32 tahun 2021 tentang penyelenggaraan bidang penerbangan," 2021.

[2] E. Poerwanto and U. Mauidzoh, "Analisis kecelakaan penerbangan di indonesia untuk peningkatan keselamatan penerbangan," *Jurnal Angkasa*, vol. VIII, no. 2, Nov. 2016.

[3] K. B, R. N, M. K. N, and G. P, "Design of iot based instrument landing system," in *2021 International Conference on Disruptive Technologies for Multi-Disciplinary Research and Applications (CENTCON)*. IEEE, Nov. 2021, pp. 207–212. [Online]. Available: https://doi.org/10.1109/CENTCON52345.2021.9688057

[4] G. Wibisono, M. Wildan, J. Wahyudi, E. Widoro, and T. Firmansyah, "Co-design structure of dual-band lna and dual-band bpf for radio navigation aid application," *Wirel Pers Commun*, vol. 116, no. 3, pp. 1659–1681, Feb 2021. [Online]. Available: https://doi.org/10.1007/s11277-020-07754-9

[5] I. C. A. Organization, "Icao's policies on charges for airports and air navigation services," 2012.

[6] F. Sabur, A. Bahrawi, and M. A. Raharjo, "Analisis pengaruh instrument landing system (ils) untuk peningkatan pelayanan keselamatan di bandar udara haluleo kendari," *Jurnal Teknik dan Keselamatan Transportasi*, vol. 3, no. 1, Jun. 2020.

[7] G. E. Berz, E. Brussels, J. Hermens, M. D. Benedetto, and A. Madsen, "Testing of ground-based radio navigation systems, 4th edition incl," 2018.

[8] M. A. Prasojo, M. Wildan, and Eriyandi, "Analisis terjadinya lost connection pada jaringan monitoring very high frequency di airnav cabang palembang," *JURNAL AMPLIFIER: JURNAL ILMIAH BIDANG TEKNIK ELEKTRO DAN KOMPUTER*, vol. 14, no. 1, pp. 95–101, May 2024. [Online]. Available: https://doi.org/10.33369/jamplifier.v14i1.34395

[9] M. P. R. Indonesia, "Peraturan menteri perhubungan nomor: Pm 29 tahun 2013 tentang penyelenggara pelayanan telekomunikasi penerbangan," 2013. [Online]. Available: www.bphn.go.id

[10] "Cns sg/24 appendix k to the report asia and pacific office asia pacific flight inspection guidance material first edition." [Online]. Available: www.icao.int

[11] J. Bredemeyer and T. Schrader, "Employing uas to perform low altitude navaids measurements," in *International Flight Inspection Symposium (IFIS)*, 2018, pp. 279–295.

[12] J. R. Sianipar, M. Wildan, and T. Firmansyah, "Design of microstrip meander line antenna for frequency resonance 332 mhz on portable ils/vor receiver for navigation aids," *Indonesian Journal of Education & Mathematical Science*, vol. 5, no. 1, pp. 12–18, 2024. [Online]. Available: https://doi.org/10.30596/ijems.v5i1.16180

[13] E. Yovita, D. Utami, N. P. Syailendra, and A. A. Febrianto, "Perancangan antena mikrostrip dual band patch persegi panjang dengan slot pada frekuensi 2,6 dan 5 ghz," *Jurnal Fokus Elektroda*, vol. 8, no. 4, pp. 264–271, 2023. [Online]. Available: https://elektroda.uho.ac.id/

[14] A. M. Nashrullah, B. S. Nugroho, and Y. Wahyu, "Perancangan dan realisasi antena mikrostrip meander line pada band uhf untuk aplikasi pembaca rfid," 2019.

[15] M. J. Arpaio, G. Paolini, F. Fuschini, A. Costanzo, and D. Masotti, "An all-in-one dual band blade antenna for ads-b and 5g communications in uav assisted wireless networks," *Sensors*, vol. 21, no. 17, p. 5734, Aug. 2021. [Online]. Available: https://doi.org/10.3390/s21175734

[16] M. A. Prasojo and M. Wildan, "Studi pengaruh perubahan dimensi groundplane dan panjang line pada antena mikrostrip meander line frekuensi 332 mhz," *Jurnal Informatika dan Teknik Elektro Terapan*, vol. 12, no. 3, Aug 2024. [Online]. Available: https://doi.org/10.23960/jitet.v12i3.4329

[17] E. Widyastuti and Susiana, "Using the addie model to develop learning material for actuarial mathematics," in *Journal of Physics: Conference Series*. Institute of Physics Publishing, Apr. 2019. [Online]. Available: https://doi.org/10.1088/1742-6596/1188/1/012052

[18] M. M. et al., "Analisis rancangan antena telemetri jenis dipole pada unmanned aerial vehicle (analysis of dipole type telemetry antenna design on unmanned aerial vehicle)," *Jurnal Teknologi Riset Terapan (JATRA)*, vol. 1, no. 2, pp. 87–95, 2023. [Online]. Available: https://doi.org/10.35912/jatra.v1i2.2404

[19] Ikhwan, R. Hayati, Misriana, and Nasri, "Analisis penambahan reflektor sudut pada antena v-double dipole pada frekuensi kerja 1.800 mhz," 2020.

[20] B. H. Bagus, T. Warsito, Y. Suprapto, R. P. Diana, T. T. dan Navigasi Udara, and P. I. P. S. J. J. Andayani, "Desain dan fabrikasi antena mikrostrip meander line $\lambda/2$ pada frekuensi vhf (very high frequency) untuk komunikasi d2d," 2018.

[21] B. Jeyapoornima, V. Chinnammal, S. Vanaja, J. J. J. Sheela, R. Krishnan, and Y. Deepika, "Design of meander line antenna for foetal movement detection," in *2021 6th International Conference on Communication and Electronics Systems (ICCES)*. IEEE, Jul. 2021, pp. 416–419. [Online]. Available: https://doi.org/10.1109/ICCES51350.2021.9489087

[22] D. Rusdiyanto, C. Apriono, and D. W. Astuti, "Analisis parameter antena mikrostrip dengan metode split ring resonator pada frekuensi l-band," *JURNAL MATRIX*, vol. 10, no. 3, 2020.

[23] N. H. Shabrina and S. Samuel, "Analisis pola radiasi antena dipole pada aplikasi wireless sensor networks di industrial site," *ULTIMA Computing*, vol. 10, no. 2, pp. 47–52, Mar. 2019. [Online]. Available: https://doi.org/10.31937/sk.v10i2.929

[24] N. A. Aboserwal, J. L. Salazar, J. A. Ortiz, J. D. Diaz, C. Fulton, and R. D. Palmer, "Source current polarization impact on the cross-polarization definition of practical antenna elements: Theory and applications," *IEEE Trans Antennas Propag*, vol. 66, no. 9, pp. 4391–4406, Sep. 2018. [Online]. Available: https://doi.org/10.1109/TAP.2018.2845945